Graefe's Arch Clin Exp Ophthalmol (2000)
238:33–39

CLINICAL INVESTIGATION

Holger Lubatschowski
Gero Maatz
Alexander Heisterkamp
Udo Hetzel
Wolfgang Drommer
Herbert Welling
Wolfgang Ertmer

Application of ultrashort laser pulses for intrastromal refractive surgery

Received: 2 February 1999
Revised version received: 7 June 1999
Accepted: 24 June 1999

H. Lubatschowski (✉) · G. Maatz
A. Heisterkamp · H. Welling
Laser Zentrum Hannover e.V.,
Hollerithallee 8, D-30419 Hanover,
Germany
e-mail: hl@lzh.de
Tel.: +49-511-2788279
Fax: +49-511-2788100

U. Hetzel · W. Drommer
Institut für Pathologie,
Tierärztliche Hochschule Hannover,
Hanover, Germany

W. Ertmer
Institut für Quantenoptik,
Universität Hannover, Hannover, Germany

Abstract ● Background: Recently, laser systems have become available which generate ultrashort laser pulses with a duration of 100–200 femtoseconds (fs). By generating microplasmas inside the corneal stroma with fs pulses, it is possible to achieve a cutting effect inside the tissue while leaving the anterior layers intact. The energy threshold to generate a micro-plasma with fs pulses is some orders of magnitude lower than it is for picosecond or nanosecond pulses. This results in a strong reduction of the thermal and mechanical damage of the surrounding tissue. ● Methods: With a titanium:sapphire fs laser system, the cutting effect on corneal tissue from freshly enucleated porcine eye globes was investigated with different pulse energies. The irradiated samples were examined by light and electron microscopy. The laser-induced pressure transients and the laser-induced bubble formation were analysed with a broadband acoustic transducer and by flash photography. ● Results: With fs laser pulses, the extent of thermal and mechanical damage of the adjacent tissue is in the order of 1 µm or below and therefore comparable with the tissue alterations after ArF excimer laser ablation. Using pulse energies of approximately 1–2 µJ and a spot diameter of 5–10 µm, intrastromal cuts can be performed very precisely in order to prepare corneal flaps and lenticules. ● Conclusion: Femtosecond photodisruption has the potential to become an attractive tool for intrastromal refractive surgery.

Introduction

Photodisruption by means of nanosecond (ns) and picosecond (ps) laser pulses is a well-known interaction process in ophthalmic surgery, introduced by Krasnov in 1974 [6] and investigated in detail by various authors [2, 17, 20, 23, 24]. Nd:YAG laser capsulotomy, for example, has become established as a standard surgical technique for treating secondary cataract [1, 3].

Photodisruption takes place when laser light is focused to power densities in the range of 10^{11}–10^{12} W/cm^2. At these intensities originally transparent material will be ionized by multi-photon absorption [20]. This process is called optical breakdown. Due to the plasma ignition and its explosive expansion, a shock wave will be generated, and if the process takes place in a fluid, a cavitation bubble develops. The extent of shock wave formation and cavitation bubble size depends on the laser pulse energy applied (Table 1). However, the aim of the surgeon is to subject the surrounding tissue to minimal mechanical stress during operation. Initial attempts at refractive corneal surgery using ps laser pulses [13, 14, 18] failed because of the strong mechanical side effects, especially the considerable bubble formation inside the corneal stroma.

Because of the threshold intensity that has to be exceeded for optical breakdown, a decrease in pulse energy can only be achieved by shortening the laser pulse duration. Recently, laser systems have become available in a more or less compact form, emitting laser pulses on the fs scale with sufficient output power. Focusing the beam

Table 1 Typical laser parameters and tissue effects for photodisruption in the ns, ps and fs regimes ([*0*] own measurements)

Parameter	ns	ps	fs
Intensity (10^{12} W/cm^2)	0.05 [23]	0.5–1 [23]	5–10 [0, 23]
Fluence (J/cm^2)	10–100 [9]	2–10 [9, 14]	1–3 [0, 9, 14]
Pulse energy (µJ)	100–10,000 [23]	1–5 [23]	0.5–3 [0, 23]
Amplitude of acoustic transient, at 1 mm distance (bar)	100–500 [21]	10–100 [21]	1–5 [0]
Diameter of cavitation bubble (µm)	1000–2000 [22]	200–500 [22]	(<100) [0]

to a spot size of some micrometres in diameter, the threshold intensity is reached at pulse energies of only 1 µJ or below. As a consequence, the secondary mechanical effects should be reduced dramatically with fs-photodisruption.

Materials and methods

The fs laser pulses are generated by a so-called Kerr lens mode-locked titanium:sapphire laser system with subsequent chirped pulse amplification [12]. The laser emits pulses at a central wavelength of 785 nm with a duration of 300 fs, measured by an autocorrelation technique. The maximum pulse energy is 1 mJ at a repetition rate of up to 1000 Hz.

The laser light was guided to a computer-controlled, two-axis scanner system and a focusing lens with 30 mm focal length (Fig. 1). On the basis of a beam diameter of 4.4 mm in front of the lens, the diameter of the laser focus (spot size) was calculated as 7 µm. Experimental confirmation was not possible at that time due to the lack of appropriate instrumentation. On the other hand, any measured value of the beam diameter which is performed in air should be interpreted carefully due to self-focusing effects inside the corneal stroma.

Freshly enucleated porcine eye globes were fixed below a suction ring with a contact glass plate on its top. The anterior segment of the cornea was slightly flattened by the bottom of the glass plate. Once the focal position inside the corneal stroma had been verified under a microscope, the glass plate was fixed to guarantee a defined location of the laser focus inside the corneal stroma for the treatment of further eyes.

For flash photography and for pressure transient measurements, the contact glass and the eye were replaced by a cuvette filled with distilled water.

The pressure measurements were performed with a calibrated PVDF hydrophone with a rise time of 4 ns [16].

For micromorphological examination, the tissue probes were fixed in glutarate dealdehyde (3.5%) and then prepared in a standardized manner for paraffin sections. The sections of 4 µm thickness were stained with haematoxylin-eosin (HE) and azan. For scanning electron microscopy (SEM) the fixed corneas were critical point dried.

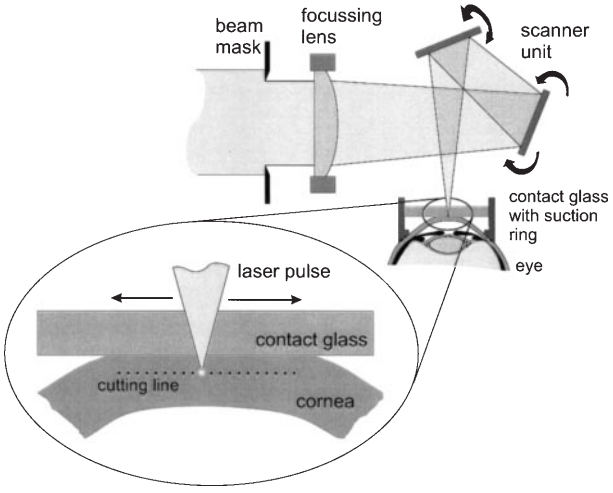

Fig. 1 Experimental setup for the beam delivery system.The laser light is guided to a scanner system and a focusing lens with 30 mm focal length. Porcine eye globes were fixed below a suction ring with a contact glass plate on its top. The glass plate has a fixed position relative to the focal plane of the laser beam. With this setup the focus of the laser beam can be well defined inside the corneal stroma

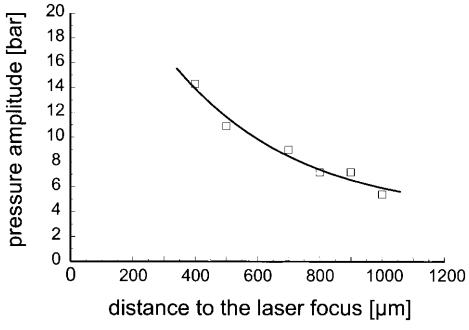

Fig. 2 Amplitude of the acoustic transients at different distances from the laser focus. According to the spherical expansion of the transients, the pressure values decrease proportional to 1/r

Results

The measured amplitudes of the laser-induced acoustic transients in water are shown in Fig. 2. The signals were recorded at a distance of 400–1000 µm from the focus of the laser pulse, where they have a full width at half maximum (FWHM) of 150 ns. The laser pulse energy was 10 µJ and the spot size was calculated to be 7 µm. According to the spherical expansion of the transients, the pressure values decrease proportional to 1/r from 14 bar at 400 µm distance to 5 bar at a distance of 1 mm.

Figure 3 shows the flash photographs of laser-induced bubbles in water for three different pulse energies. The laser was scanned from left to right with a spot separation of 200 µm and a repetition rate of 1 kHz. The expo-

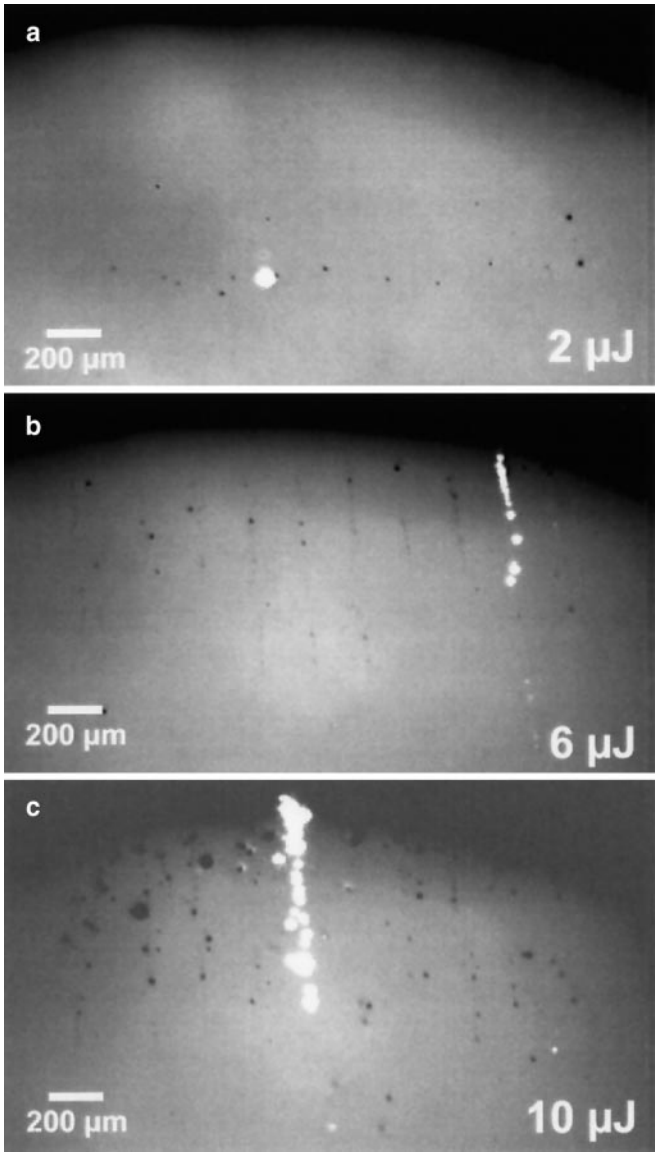

Fig. 3a–c Shadowgraphs of laser-induced bubbles in water for three different pulse energies. The 300-fs laser pulses were scanned from left to right with a spot separation of 200 µm and a repetition rate of 1 kHz. The exposure time for the camera was 20 ns. The bright spots in the centre of the pictures are caused by laser light scattered at the gas bubbles. Plasma luminescence could not be observed in any of the photographs

sure time for the camera was 20 ns. In Fig. 3a, with an incident laser pulse energy of 2 µJ, the shadows of a bubble chain in the focal area of the laser can be seen. The bubbles have a diameter of approximately 25 µm. The bright spot in the centre of the picture is caused by laser light scattered at the gas bubble. It should be noted that no plasma luminescence can be observed in any of the photographs. It is also remarkable that almost no bubble dynamics in terms of expansion and collapsing could be recognized. All the bubbles in the photograph have almost the same size despite being generated one after another at intervals of 1 ms due to the repetition rate of 1 kHz. At longer exposure times the gas bubbles slowly rise while maintaining their size.

In Fig. 3b, the laser pulse energy was increased to 6 µJ. Obviously, the threshold condition for bubble generation is already fulfilled before the laser intensity has reached its maximum in the focal plane. However, the laser energy is not fully dissipated after the first bubble generation, thus leading to a vertical chain of laser-induced gas bubbles.

At 10 µJ pulse energy (Fig. 3c) the secondary effects caused by optical breakdown are strong enough to produce larger bubbles with diameters up to 100 µm.

The mechanical and thermal side effects of the laser energy on the irradiated tissue are illustrated by the histological sections (Figs. 4, 5). Figure 4 shows a section of a porcine cornea, irradiated with a series of 300-fs pulses with a pulse energy of 4 µJ. The spot size was expected to be 7 µm. The spot separation during the scan was 15 µm. On the right, the laser focus was moved upwards into the epithelium. Although optical breakdown took place inside the epithelium, no denudation or bursting of the epithelial layer could be observed.

Both mechanical and thermal side effects caused by laser interaction are relatively minor. Both in azan staining (Fig. 4) and in HE staining (Fig. 5) the zone of visible thermal alteration of adjacent tissue is of the order of 1 µm. Only inside the bubbles is loose debris of the collagen, being directly in the interaction zone of the laser pulse, completely coagulated.

Femtosecond photodisruption offers the possibility to perform a refractive surgical operation by preparing an intrastromal lenticule, analogous to LASIK, without using a mechanical microkeratome [4, 7].

The principle of this procedure is shown in Fig. 6. In a first step, a lamellar intrastromal cut is performed by scanning the laser in a spiral pattern. This procedure is analogous to the mechanical cut of a microkeratome in the conventional LASIK procedure. In a second step, another cut prepares a lenticule with the desired shape, depending on the refractive error of the treated eye. Only in the third step, the anterior corneal flap is opened, and the prepared lenticule can be extracted. Finally, the flap will be repositioned on the cornea. The surface of the cornea follows the missing volume of the lenticule, thereby leading to a change in refractive power.

On the scanning electron micrograph in Fig. 7, a treated cornea with an opened flap is shown. The lenticule was displaced for better demonstration. The laser had an energy of 1.5 µJ/pulse with a spot size of 7 µm. The spot separation during the spiral scans was 8 µm.

With the same laser parameters a flap of 300 µm thickness was created in another cornea to demonstrate the quality of the cut edge of the remaining corneal tis-

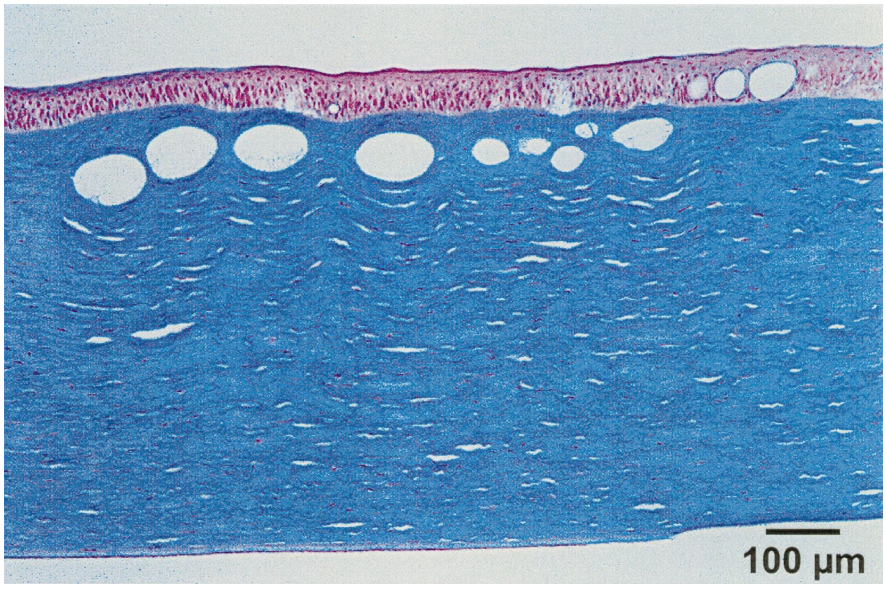

Fig. 4 Histological section (azan staining) of a porcine cornea irradiated with a series of 300-fs pulses with a pulse energy of 4 µJ. The focal spot had a diameter of 7 µm. The spot separation during the scan was 15 µm. On the right, the laser focus was moved upwards into the epithelium. Although optical breakdown takes place inside the epithelium, no denudation or bursting of the epithelial layer could be observed

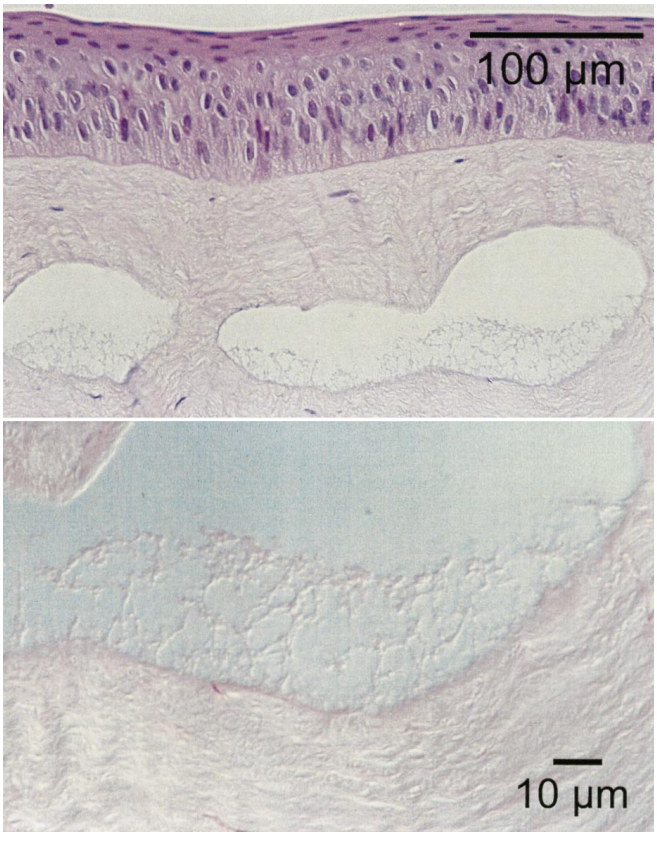

Fig. 5a,b Histological section with HE staining. The cornea was irradiated with the same laser parameters described in Fig. 4. The zone of visible thermal alteration of the adjacent tissue is of the order of 1 µm. **b** Inside the bubbles, loose debris of the collagen in the interaction zone of the laser pulse can be seen. (In eyes fixated upside down, the debris sedimented inside the bubble to the anterior side of the cornea)

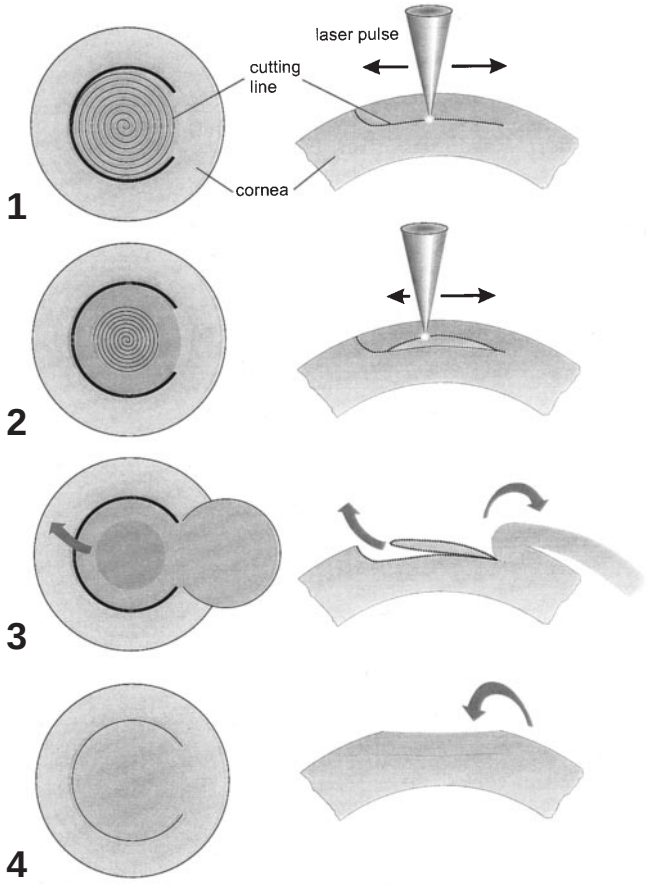

Fig. 6 Principle of fs laser keratomileusis. In a first step, a lamellar intrastromal cut is performed by scanning the laser in a spiral pattern. In a second step, another cut prepares a lenticule with the desired shape, depending on the refractive error of the treated eye. Only at the third step is the anterior corneal flap opened and the prepared lenticule extracted. Finally, the flap is repositioned on the cornea. The surface of the cornea follows the missing volume of the lenticule, leading to a change in refractive power

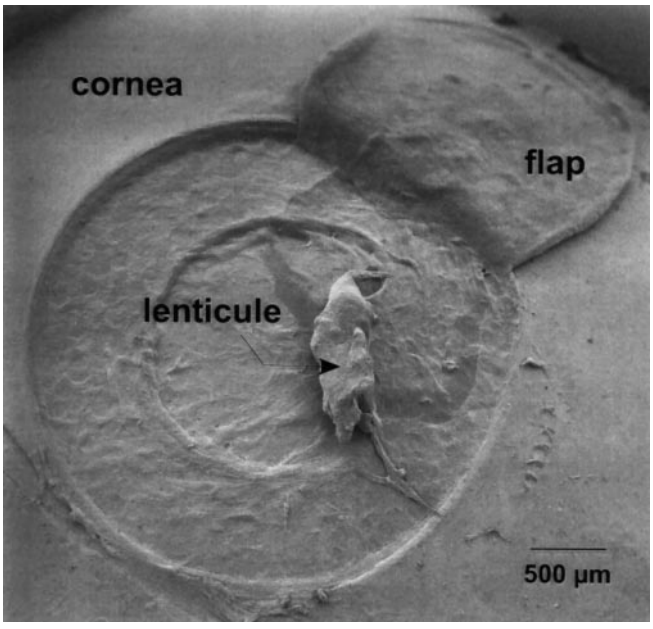

Fig. 7 Scanning electron micrograph of a prepared intrastromal lenticule with fs laser pulses.The corneal flap is opened and the lenticule displaced for better demonstration. The laser had an energy of 1.5 µJ/pulse with a focal spot diameter of 7 µm. The spot separation during the spiral scans was 8 µm

sue (Fig. 8). The vertical cut of the cylinder was created by scanning the focus on rings at decreasing depth inside the cornea.

The surface quality of the treated corneal stroma is shown in Fig. 9. Again, the same laser parameters were used. The thickness of the flap is approximately 100 µm. At high magnification, the stromal fibrils can be identified. This again is a strong indication for the weak thermal effect of fs photodisruption on corneal tissue.

Discussion

Although non-linear acoustic effects are expected close to the range of laser-induced optical breakdown [15], the mechanical damage to the surrounding tissue is rather slight when ultrashort laser pulses are applied. The amplitudes of the acoustic transients generated by fs laser pulses are more than one order of magnitude lower than those generated by ps or ns optical breakdown [21] or by excimer or erbium laser photoablation [5, 11, 19]. Moreover, in this study the pressure measurements were performed at laser pulse energies of 10 µJ, which is probably 5–10 times higher than clinically relevant pulse energies. However, detection of smaller amplitudes was beyond the capability of the calibrated hydrophone.

The detected acoustic transients have a FWHM of 150 ns, about six orders of magnitude longer than the laser pulse itself and still 40 times longer than the rise time

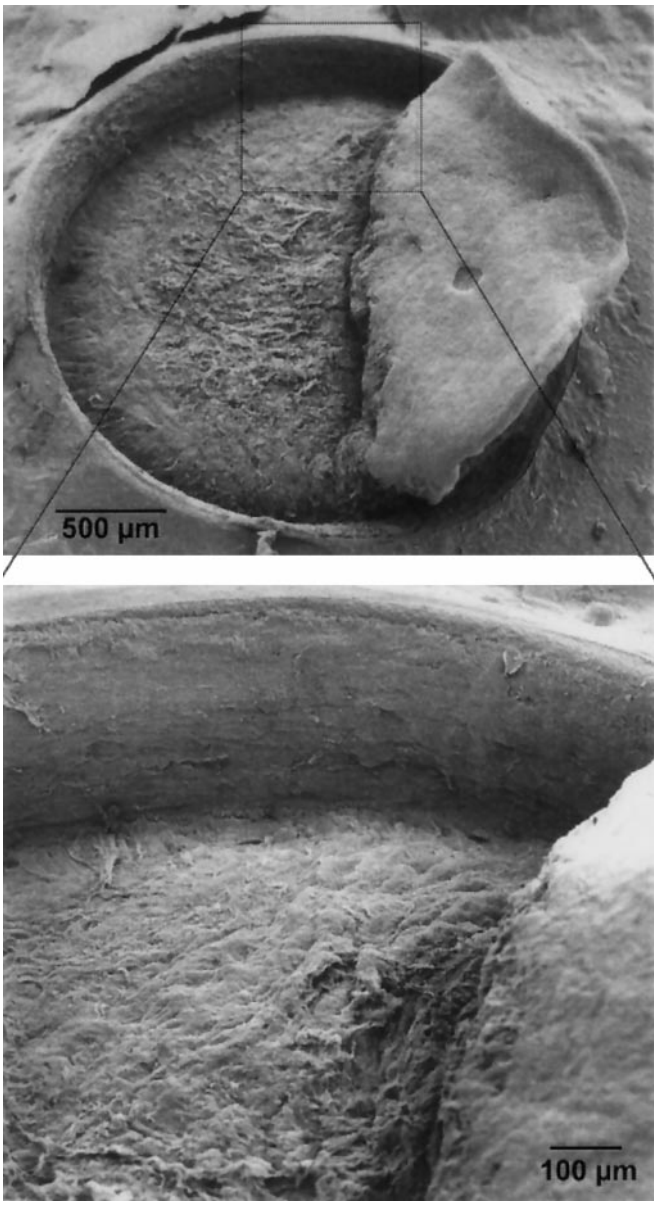

Fig. 8 Lamellar keratoplasty performed with the same laser parameters used in Fig. 7. The wall of the cylinder was created by scanning the focus on rings at decreasing depth inside the cornea

of the hydrophone. The reason for the broadening is not yet clear and can be manifold. On one hand it is known that acoustic transients are broadened by acoustic dispersion and diffraction [10]. On the other hand the wavefront of the transients has a radius of curvature which is comparable to the diameter of the active area of the hydrophone. This leads to signal distortion. Finally, the acoustic transients are generated over a long distance due to multiple optical breakdown at higher pulse energies (see Fig. 3). Thus the superposition of the single transients could lead to spatial and temporal broadening.

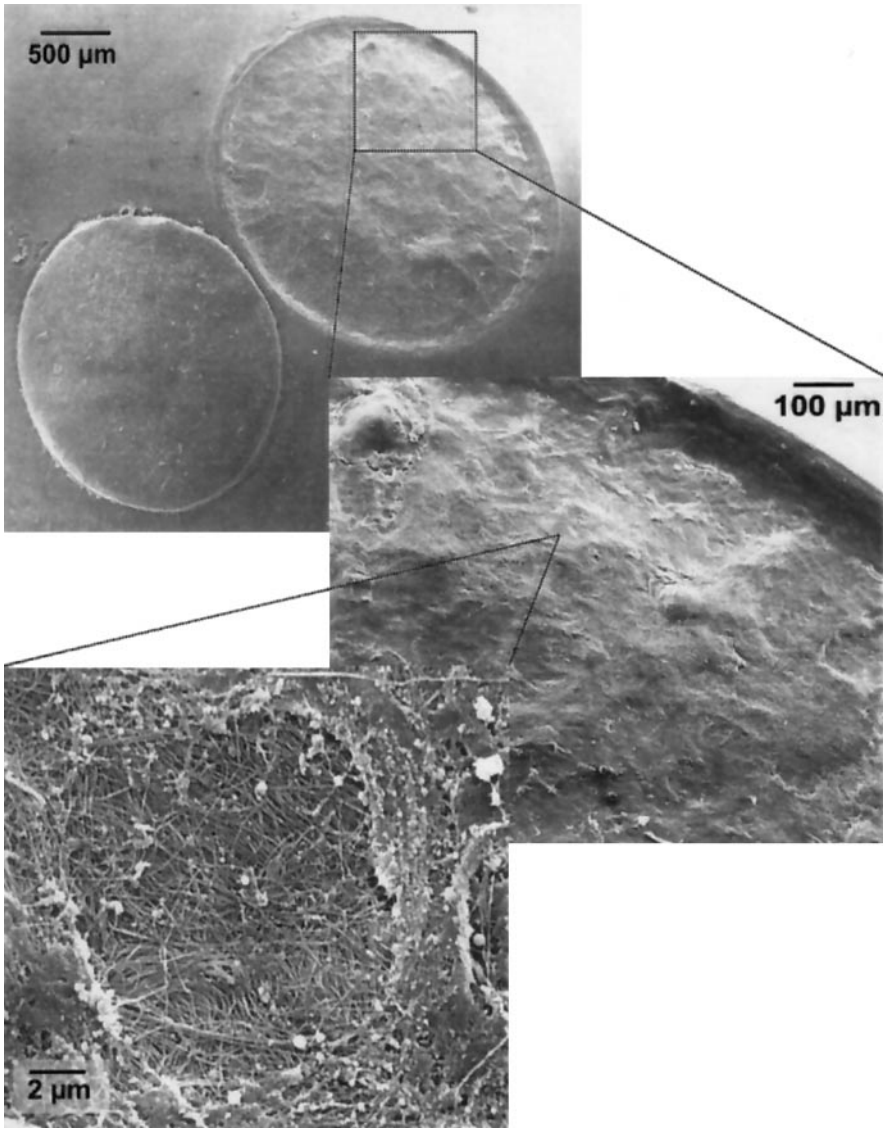

Fig. 9 Scanning electron micrographs of a prepared corneal flap to demonstrate the surface quality of the corneal stroma after fs laser interaction. Same laser parameters as in Fig. 7. At high magnification, the stromal fibrils can be identified

The laser-induced bubble dynamics at pulse energies close to threshold apparently differs from the cavitation process which is known for ns and ps laser pulses. The maximum diameter of the detected bubbles is of the order of 10 µm. Since they maintain their size, we expect them to be gas-filled bubbles instead of cavitation bubbles. The analysis of the gas is subject of current investigations and will be reported elsewhere. In any case, the photographs in Fig. 3 show that it is important to operate close to the threshold of optical breakdown. Otherwise, multiple optical beakdown will prevent a smooth intrastromal cut.

The relatively large bubbles presented in the histological sections of the corneal stroma (Figs. 4, 5) are created by the merging of many single bubbles of different laser pulses close to another within the same layer of the stromal fibrils. If the eyes are not subjected to fixation agents after laser processing, the bubbles disappear within 10–15 min.

The dynamics of the bubbles, their interaction with each other and, especially, their influence on the laser focus is unclear and has to be analysed in future studies. Certainly they determine the quality of the laser cut. Due to the lamellar structure of the corneal stroma, they prefer to expand horizontally. This might be the reason why the quality of the vertical cut appears smoother than the surface of the opened corneal stroma.

Obviously, pulse energy of 1.5 µJ, spot size of 7 µm and spot separation of 8 µm are parameters well suited for preparing lamellar dissections. To remove the prepared lenticule, gentle traction was needed to break residual adhesions of the collagen fibrils. Kurtz et al. [8] found similar parameters for producing a smooth intrastromal cut, except that they required a higher pulse en-

ergy (8 µJ). Despite all efforts, optimal cutting parameters have still to be ascertained by systematic parameter variation.

For myopic correction, where only little material has to be removed, the lenticule will inevitably become very thin at the edge. So, the crucial question is: To what precision can the intrastromal cut be performed, and what is the minimal thickness of the lenticule? On this the spectrum of clinical applications might ultimately depend. Furthermore, animal studies and blind eye studies have to demonstrate that the wound healing of the treated corneal tissue takes a course comparable, in terms of regression and reproducibility, to that known from ArF excimer laser surgery.

In conclusion, mechanical and thermal side effects caused by fs photodisruption are comparable to what is known from excimer laser ablation. Cavitation, which causes difficulties when using ns and ps laser pulses, is reduced dramatically. Thus, intrastromal refractive surgery is feasible. However, laser parameters such as pulse energy, spot size and scanning procedure have to be optimized for clinical applications. In the same way, the accuracy and reproducibility of the refractive outcome on living eyes have to be investigated, as well as the postoperative wound healing process and regression. In the expectation of small and compact laser sources, fs photodisruption has the potential to be an attractive tool for intrastromal refractive surgery.

References

1. Aron-Rosa D, Aron JJ, Griesemann M, Thyzel R (1980) Use of the Nd:YAG laser to open the posterior capsule after lens implant surgery: a preliminary report. Am Intraocul Implant Soc J 6:352
2. Birngruber R, Puliafito CA, Gawande A, Lin WZ, Schoenlein RW, Fujimoto JG (1987) Femtosecond laser-tissue interaction: retinal injury studies. IEEE J Quant Electron QE-23:1836–1844
3. Fankhauser F, Roussel P, Steffen J, van der Zypen E, Chrenkova A (1981) Clinical studies on the efficiency of a high power laser radiation upn some structures of the anterior segment of the rabbit eye lens. Int Ophthalmol Clin 3:129–139
4. Ito M, Quantock AJ, Malhan S, Schanzlin DJ, Krueger RR (1996) Picosecond laser in situ keratomileusis with a 1053-nm Nd:YLF laser. J Refract Surg 12:721–728
5. Kermani O, Lubatschowski H (1991) Struktur und Dynamik photoakustischer Schockwellen bei der 193 nm Excimerlaserphotoablation der Hornhaut. Fortschr Ophthalmol 88:748–753
6. Krasnov MM (1974) Q–switched laser goniopuncture. Arch Ophthalmol 92:37–41
7. Krueger RR, Juhasz T, Gualano A, Marchi V (1998) The picosecond laser for nonmechanical laser in situ keratomileusis. J Refract Surg 14:467–469
8. Kurtz RM, Horvath C, Liu HH, Juhasz T (1998) Optimal laser parameters for intrastromal corneal surgery. SPIE 3255:56–66
9. Loesel FH, Niemz MH, Horva HC, Juhasz T, Bille JF (1997) Experimental and theoretical investigations on threshold parameters of laser-induced optical breakdown on tissues. Proc SPIE 2923:118–126
10. Lohmann S, Ruff C, Schmitz C, Lubatschowski H, Ertmer W (1997) Photoacoustic determination of optical parameters of tissue-like media. Lasers Med Sci 12:357–363
11. Lubatschowski H, Högele A, Lohmann S, Olmes A, Ertmer W (1996) Erbium-laser photoablation of the cornea. Proc SPIE 2930:2–8
12. Morou G (1997) The ultrahigh-peak power laser: present and future. Appl Phys B 65:205–211
13. Niemz MH, Klancnik EG, Bille JF (1991) Plasma-mediated ablation of corneal tissue at 1053 nm using a Nd:YLF oscillator/regenerative amplifier laser. Lasers Surg Med 11:426–431
14. Niemz MH, Hoppeler TP, Juhasz T, Bille JF (1993) Intrastromal ablations for refractive corneal surgery using picosecond infrared laser pulses. Lasers Light Ophthalmol 5:149–155
15. Noack A, Hammer DX, Noajin GD, Rockwell BA, Vogel A (1998) Influence of pulse duration on mechanical effects after laser-induced breakdown in water. J Appl Phys 89:7488–7495
16. Olmes A, Lohmann S, Lubatschowski H, Ertmer W (1997) An improved method of measuring laser induced pressure transients. Appl Phys B 64:677–682
17. Puliafito CA, Steinert RF (1984) Short-pulsed Nd:YAG laser microsurgery of the eye: biophysical considerations. IEEE J Quant Electon QE-20:1442–1448
18. Remmel M, Dardenne CM, Bille JF (1992) Intrastromal tissue removal using an infrared picosecond Nd:YLF ophthalmic laser operating at 1053 nm. Lasers Opthalmol 4:169–173
19. Rossi F, Pini R, Siano S, Salimbeni R (1996) Imaging of acoustic waves induced by excimer laser ablation of the cornea. Proc SPIE 2930:58–62
20. Vogel A (1997) Nonlinear absorption: intraocular microsurgery and laser lithotripsy. Phys Med Biol 42:895–912
21. Vogel A, Busch R (1996) Shock wave emission and cavitation bubble generation by picosecond and nanosecond optical breakdown in water. J Acoust Soc Am 100:148–165
22. Vogel A, Busch S, Asio-Vogel M (1993) Time-resolved measurements of shock-wave emission and cavitation-bubble generation in intraocular laser surgery with ps- and ns-pulses and related tissue effects. Proc SPIE 1877:312–322
23. Vogel A, Noack A, Nahen K, Theisen D, Birngruber R, Hammer DX, Noojin GD, Rockwell BA (1998) Laser-induced breakdown in the eye at pulse durations from 80 ns to 100 fs. SPIE 3255:43–49
24. Zysset B, Fujimoto JG, Puliafito CA, Birngruber R, Deutsch TF (1989) Picosecond optical breakdown: tissue effects and reduction of collateral damage. Lasers Surg Med 9:193–204